

Magnetic ordering in the charge-ordered Nb₁₂O₂₉

Alexandros Lappas

Institute of Electronic Structure and Laser, Foundation for Research and Technology-Hellas, P.O. Box 1527, 711 10 Heraklion, Greece

Joanna E. L. Waldron and Mark A. Green*

Royal Institution of Great Britain, 21 Albemarle Street, London W1X 4BS, United Kingdom

and Department of Chemistry, University College London, Christopher Ingold Laboratories, 20 Gordon Street, London WC1H 0AJ, United Kingdom

Kosmas Prassides

School of Chemistry, Physics and Environmental Sciences, University of Sussex, Falmer, Brighton BN1 9QJ, United Kingdom

and Institute of Materials Science, NCSR "Demokritos," 15310 Ag. Paraskevi, Athens, Greece

(Received 23 August 2001; published 13 March 2002)

Magnetic susceptibility and zero-field muon spectroscopy (ZF- μ^+ SR) measurements of monoclinic Nb₁₂O₂₉ are reported. The magnetic susceptibility shows a broad maximum at around 12 K with no divergence between the zero-field cooled and field-cooled susceptibility, implying low-dimensional antiferromagnetic ordering. Application of the Bonner-Fischer model, applicable for a uniform $S = \frac{1}{2}$ linear Heisenberg chain, gives an exchange energy of $J/k = 12.71$ K and substantially reduced $g = 0.556$. In this magnetically dilute system, the observation of an oscillating signal in the ZF- μ^+ SR experiments is a clear and unambiguous signature of static magnetic correlations. We argue that this is due to an incommensurate arrangement of the Nb⁴⁺ electronic moments, similar to a spin-density wave. This phase sets in below $T_f \approx 10$ K and produces spontaneous muon-spin precession associated with two distinct internal local fields that saturate at 39.3(6) and 138(1) G at 60 mK.

DOI: 10.1103/PhysRevB.65.134405

PACS number(s): 75.30.Kz, 74.25.Ha, 71.20.Be

Charge ordering in mixed-valency systems has become increasingly important in the understanding of the electronic properties of many transition metal and post-transition metal oxides. This phenomenon, where different metal oxidation states adopt crystallographically distinct sites, has been shown to occur in a number of systems. For example, it causes unusual "charge stripes" in lanthanide nickelates¹ and creates both commensurate and incommensurate states in the Ba_{1-x}K_xBiO₃ superconductors.² Charge ordering can have a dramatic effect on the electronic characteristics of the system, for example, a metal-insulator transition in some manganese perovskites is caused by localization of Mn³⁺ and Mn⁴⁺ ions onto specific sites.³ Charge ordering is particularly intriguing in d^0/d^1 systems, where the possibility of controlling the ratio of magnetic ($d^1, S = \frac{1}{2}$) and diamagnetic ($d^0, S = 0$) ions, provides the opportunity to manipulate and tailor new magnetic structures.

Low-temperature powder neutron diffraction has recently been used to reveal a complex charge ordering transition in monoclinic Nb₁₂O₂₉. It was shown that between 5 and 25 K, within which there is also a maximum in the magnetic susceptibility, one unpaired electron localizes onto a specific crystallographic site within the (4×3) block structure. This gives rise to a unique one-dimensional structural arrangement of Nb⁴⁺ ions.⁴ Nb₁₂O₂₉ can be written as Nb₂⁴⁺Nb₁₀⁵⁺O₂₉, therefore containing two unpaired electrons per formula unit. The second unpaired electron contributes to metallic conduction in this system, as also noted for the orthorhombic analog.⁵ The most likely magnetic state for

a localized electron randomly embedded in a sea of conduction electrons is the formation of a spin glass state. However, it is this site randomness in certain systems, such as CuMn, which is necessary to produce the spin glass properties.⁶ The unpaired electron localized onto a specific site in Nb₁₂O₂₉ gives an intriguing possibility of a unique form of low-dimensional magnetism. The structure of monoclinic Nb₁₂O₂₉ in the charge-ordered state, is shown in Fig. 1.⁴ It shows chains of Nb⁴⁺ ions with equivalent nearest-neighbor chains 15.1, 15.7, or 10.5 Å apart; an extremely large distance for a condensed phase system. Many low-dimensional

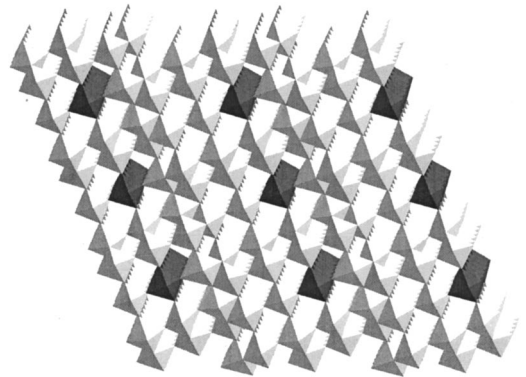


FIG. 1. An illustration of the structure of the monoclinic Nb₁₂O₂₉. The projection to the (100) lattice plane is shown and with the Nb⁴⁺ ($S = \frac{1}{2}$) crystal sites darkly shaded, and the Nb⁵⁺ ($S = 0$) ones lightly shaded.

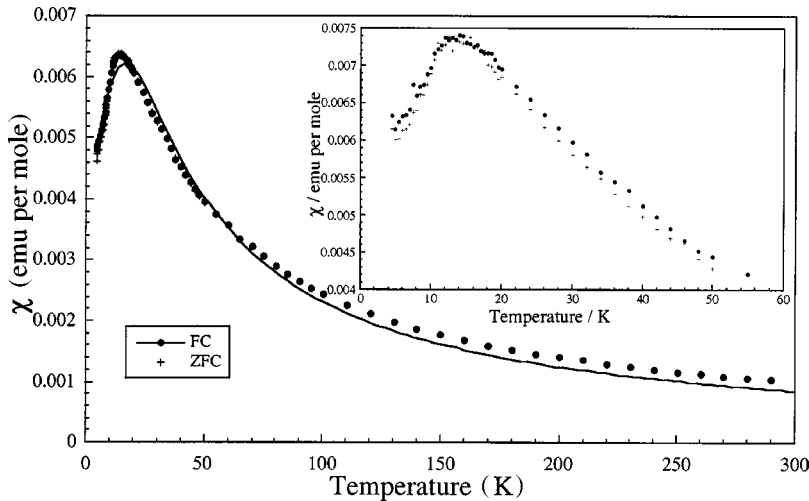


FIG. 2. The zero-field cooled and field cooled molar magnetic susceptibility of monoclinic $\text{Nb}_{12}\text{O}_{29}$ performed in an applied field of 100 G in the temperature range of 1.8–300 K. The solid curve shows the fit to the Bonner-Fischer model. The inset shows the same experiments performed in an applied field of 10 G from 1.8–60 K.

magnetic structures are known, such as SrCu_2O_3 ; however, the distance between chains is usually relatively small (<4 Å) which causes a significant amount of interchain interaction, often leading to magnetic frustration. The formation of magnetic chains in the condensed phase of $\text{Nb}_{12}\text{O}_{29}$, which are well spaced apart is more typical structural arrangement in molecular magnet systems.⁷ However, condensed phase systems allow for much greater chemical manipulation and control, for example, in the alteration of the number of unpaired electrons, through the ability to easily dope the system. The complexity of the magnetic state in $\text{Nb}_{12}\text{O}_{29}$ also suggests the existence of a number of new magnetic structures in systems containing mixtures of d^0 and d^1 ions.

To investigate the nature of the magnetic transition in monoclinic $\text{Nb}_{12}\text{O}_{29}$, a series of magnetic susceptibility and zero-field muon spectroscopy (ZF- μ^+ SR) measurements have been performed. We show that the magnetic transition at 12 K in monoclinic $\text{Nb}_{12}\text{O}_{29}$ is associated with long-range antiferromagnetic ordering. This is evident in the overlap of zero-field-cooled and field-cooled magnetic susceptibility data and is strengthened by the observation of two distinct oscillations in the ZF- μ^+ SR spectra. The oscillations were modelled using an exponentially damped Bessel function appropriate for such a dilute magnetic system. Furthermore, the Bessel function used in the fitting is consistent with the oscillating nature of the interaction, which we suggest originates from the RKKY interaction between the chains mediated through the conduction electrons.

Monoclinic $\text{Nb}_{12}\text{O}_{29}$ was synthesized from $\text{H-Nb}_2\text{O}_5$ and Nb metal in a sealed evacuated quartz tube at a temperature of 1200 °C for 1 h, followed by rapid quenching to room temperature. $\text{H-Nb}_2\text{O}_5$, was first formed by firing as supplied Nb_2O_5 at 1100 °C for 24 h. The phase purity was confirmed through Rietveld refinement of x-ray and neutron powder diffraction data.⁴ Magnetic susceptibility measurements were performed using a Quantum Design MPMS7 SQUID magnetometer. Measurements were carried out in applied fields of 10, 100, and 1000 G from 1.8–300 K, following both a zero-field-cooled (ZFC) and field-cooled (FC) procedure. The μ^+ SR data in zero field (ZF) were collected on the LTF spectrometer of the μ^+ SR-dedicated πM3 beam-

line, on the 600 MeV proton accelerator at the Paul Scherrer Institute, Villigen, Switzerland. The instrument was employing a $^3\text{He-}^4\text{He}$ dilution refrigerator to access the millikelvin temperature regime. Pressed pellets of the powdered samples were attached with low-temperature varnish on a Pt sample-holder placed on the sample stick of the dilution refrigerator. 100% spin-polarized positive muons were implanted in the solid sample and, after they come to rest at an interstitial lattice site, they act as highly sensitive microscopic local magnetic probes. The μSR technique in its various variants has proven extremely powerful in the field of small-moment magnetism, and in all cases, when magnetic order is of random, very short-range, spatially inhomogeneous or incommensurate nature.⁸ ZF- μ^+ SR data for $\text{Nb}_{12}\text{O}_{29}$ were collected on the LTF spectrometer at various temperatures between 0.060 and 14 K.

The ZFC and FC magnetic susceptibility of monoclinic $\text{Nb}_{12}\text{O}_{29}$ in an applied field of 100 G and in the temperature range of 1.8–300 K is shown in Fig. 2. The inset shows the equivalent measurements from 1.8–60 K in an applied field of 10 G. The measurements show a broad maximum in the magnetic susceptibility around 12 K, often an indication of low-dimensional anti-ferromagnetic behavior. Both the 100 and 10 G measurements show no deviation between the ZFC and FC measurements, which would have indicated spin-glass character, giving strong evidence for long-range magnetic order. Although this observation is unusual in such a dilute magnetic spin system, previous structural work has reported the structural ordering of the Nb^{4+} ($S = \frac{1}{2}$) ions onto a specific site,⁴ as shown in Fig. 1. The maximum in the susceptibility is, therefore, a consequence of three-dimensional ordering of the magnetic chains. Magnetic susceptibility of a uniform $S = \frac{1}{2}$ linear Heisenberg chain is theoretically described by the Bonner-Fischer model,⁹ given below:

$$\chi_M = \frac{(Ng^2\mu_B^2)}{kT} \left(\frac{A + Bx + Cx^2}{1 + D + Ex^2 + Fx^3} \right), \quad (1)$$

where $x = |J|/kT$, $A = 0.25$, $B = 0.14995$, $C = 0.30094$, $D = 1.9862$, $E = 0.68854$, and $F = 6.0626$.

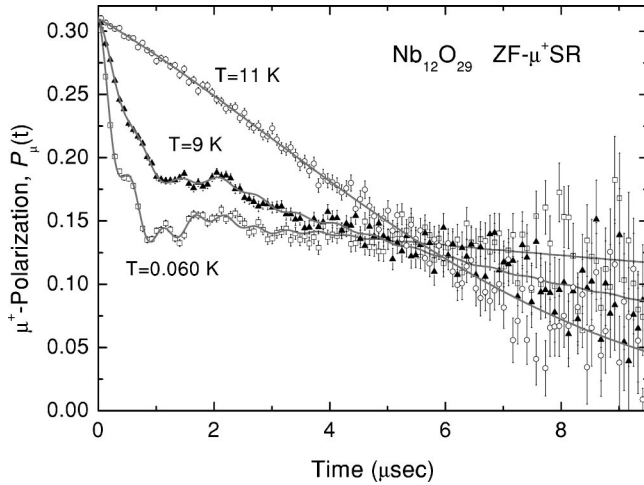


FIG. 3. Time-dependent muon-spin relaxation spectra at zero-field for monoclinic Nb₁₂O₂₉. Clear evidence for long range magnetic order is reflected in the coherent μ^+ -spin precession (wiggling) signal, seen below $T_f \cong 10$ K.

The fitting using this model in the 1.8–300 K temperature regime is shown in Fig. 2, and provides values of $J/k = 12.71$ K and $g = 0.556$. The value of g is significantly lower than the value of 2 for insulating systems with zero spin-orbit coupling. Both the metallic nature of the system and strong spin-orbit coupling will greatly affect the value of g . The fit to the observed susceptibility is satisfactory; however, the crystal structure above the magnetic transition⁴ has shown that the charge ordering does not occur in this temperature regime, implying that the charge ordering of the mixed valency ions is possibly concomitant with the three dimensional magnetic transition. Therefore, the spins are not aligned in a chain, but are somewhat randomly distributed. A Curie-Weiss fit to the high-temperature data, which includes a temperature independent paramagnetic term to account for the conduction electrons and a diamagnetic core, yields values of $C = 0.3209$ emu K mol⁻¹ and $\theta = -26.36$ K. The observed effective moment μ_{eff} is calculated to be $0.66\mu_B$, around 48% of that expected from the spin-only contribution to the magnetic susceptibility. This clearly indicates that the electrons are still localized above the charge-ordering transition; however, as there is no structural evidence for charge ordering in this temperature regime the localized electrons are presumably distributed over all Nb sites or possibly a subset of preferred sites.⁴ The fact that the spins are not aligned in chains above their ordering temperature, indicates that the anomaly at 12 K is the combination of a magnetic and charge ordering transition, and the form of the Bonner-Fischer function may not be appropriate.

In the absence of an external field, the appearance of a precession in the time-dependent μ^+ SR spectra signals the onset of a magnetic ordering transition. This is because the μ^+ spin undergoes Larmor precession, with a frequency $\nu_\mu = (\gamma_\mu/2\pi)\langle B_\mu \rangle$ (where $\gamma_\mu/2\pi = 13.55$ kHz/G is the muon gyromagnetic ratio), due to nonzero local magnetic fields of strength $\langle B_\mu \rangle$. A system in a frozen spin-glass state, due to short-range random static magnetism, does not show oscillatory behavior in the ZF- μ SR signal. The precession signal

(Fig. 3) observed in the zero-field muon polarization below 11 K is definitive proof of long-range coherent static arrangement of moments. These oscillations vanish gradually upon heating causing a change in the line shape of the relaxation to being more Gaussian-like character. The transition is consistent with the observed maximum in the magnetic susceptibility of the Nb₁₂O₂₉ at around 12 K. Figure 3 shows representative time-dependent muon spectra at selected temperatures above and below the spin-freezing transition at $T_f < 11$ K. The nonoscillating signal at $T \geq 11$ K was best fitted by the product of a Lorentzian and Gaussian relaxation function

$$P_\mu(t) = A \exp(-\lambda t) \exp(-1/2\sigma^2 t^2), \quad (2)$$

where A is the magnitude of the asymmetry, and λ and σ are the associated damping rates. The physical origin of this μ^+ -spin relaxation rests on arguments of coexisting relaxation mechanisms in the same sample volume. That is, slowly fluctuating electronic moments act as an independent channel of depolarization in addition to the dipolar fields arising from the randomly frozen nuclear spins at the Nb sites. The latter term has an almost temperature-independent relaxation rate of $\langle \sigma \rangle = 0.19(2) \mu\text{s}^{-1}$, and is responsible for producing a field distribution with a width of $\langle \Delta B^2 \rangle^{1/2} \cong 2.2(2)$ G. At the same time the electronic spins appear to be slowing down on cooling, since λ increases from $0.041(4) \mu\text{s}^{-1}$ at 14 K to $0.086(4) \mu\text{s}^{-1}$ at 11 K. This behavior, as T_f is approached from above, is a precursor to the static spin freezing at lower temperatures.

The shape of the oscillatory muon-polarization signal incorporates two contributions and is generally modelled by $P_\mu(t) = P_z(0) G_\perp(t) \cos(2\pi\nu_\mu t) + P_x(0) G_\parallel(t)$, where $P_z(0)$ and $P_x(0)$ are the amplitudes of transverse and longitudinal initial ($t=0$) polarizations. The theory predicts that if the local magnetic fields are purely static, then only $\frac{2}{3}$ of the initial amplitude of the muon ensemble polarization will perform Larmor precession with frequency ν_μ and the volume fractions will follow the ideal ratio $P_x(0)/P_z(0) = \frac{1}{2}$. Its physical origin lies with the fact that on average, for a completely random distribution of the directions of the internal field in a homogeneous powder sample, one-third of all muons experiences an internal field along their initial spin direction and do not precess. The previous ideal ratio does not always hold in real chemical systems where internal field inhomogeneities are present. Temporal fluctuations or randomness of the local field at the muon site are expected to incorporate time-evolution in the $\frac{2}{3}$ and/or $\frac{1}{3}$ terms, thus explaining the origin of time dependence in $P_\mu(t)$ and the necessity of $G_\perp(t)$ and $G_\parallel(t)$ functions in the mathematical description of muon depolarization. Each one of the $G_\perp(t)$ and $G_\parallel(t)$ relaxation functions is associated with a part of the sample volume and for this reason their exact form is very informative regarding the microscopic physical mechanisms responsible for the muon-spin depolarization.

More specifically to account for the $G_\perp(t)$ and $G_\parallel(t)$ terms in fitting the ZF- μ^+ SR data of Nb₁₂O₂₉, the following phenomenological function was used:

$$P_{\mu}(t) = [A_{\perp}^{\perp} \exp(-\lambda_1 t) J_0(2\pi\nu_1 t) + A_{\perp}^{\parallel} \exp(-\lambda_2 t) J_0(2\pi\nu_2 t)] + A_3^{\parallel} \exp(-\lambda_3 t) \quad (3)$$

shown as a solid line through the data in Fig. 3. A_{\perp} and A_{\parallel} are amplitudes reflecting the fractions ($A_{\perp} + A_{\parallel} = 1$) of the muons contributing to the depolarization of the muon spin, ν_1 , ν_2 are the Larmor frequencies of the coherent μ^+ spin precession, whereas λ_1 , λ_2 represent relaxation rates due to field components perpendicular to the μ^+ spin, and λ_3 reflects relaxation associated to both dynamic and static field inhomogeneities along the μ^+ -spin direction. The use of the damped J_0 -Bessel function to describe the oscillations was preferred over the simple oscillating term $P_{\mu}(t) \sim \exp(-\lambda t) \cos(2\pi\nu_{\mu} t + \phi)$ because the latter led to unphysically large values¹⁰ of 18° – 45° for the phase ϕ . The spontaneous signal in $\text{Nb}_{12}\text{O}_{29}$ is described by two oscillating components Nos. 1 and 2. We will attempt to rationalize this in the following paragraphs. As we mentioned above, the third term, in Eq. (2), accounts for the fact that on average, for a completely random distribution of the directions of the local field in a polycrystalline compound, one-third of all muons experience an internal field along their initial spin direction. As a consequence, they will not precess, but will contribute to the $\exp(-\lambda_3 t)$ term.

In the adopted model [Eq. (3)], the use of the Lorentzian (λ) over the Gaussian (σ) term in the damping functions, is justified by the dilute nature of the magnetic system. The chemical formula can be written as $\text{Nb}_2^{4+}\text{Nb}_{10}^{5+}\text{O}_{29}$, with only one site of the two Nb^{4+} (d^1) localized per formula unit of twelve niobium ions. For such a dilute spin system, a Lorentzian function describes appropriately local fields with a $1/r^3$ interaction, where r is the distance between the moment and the muon site.¹¹ In the case of a long-range ordered magnetic state, the muon experiences the moment (or otherwise an internal field) of a unique magnitude, originating from several static ordered moments, but in a dilute spin system the associated oscillating term acquires some damping due to the internal magnetic field distribution. In the more general case, this is due to the fact that different muon sites are in different surrounding moment configurations, with some having nearby moments and others without any. The local field then has a much wider spread than that described by a Gaussian function, which represents the field distribution in concentrated spin systems. A number of different fitting procedures was evaluated, but the functional form of Eq. (3), with an exponential damping, proved superior in appropriately accounting for the high concentration of diamagnetic Nb^{5+} (d^0) ions.

The observation of ν_{μ} in zero external field is a undisputable evidence for the spontaneous ordering of the electronic Nb^{4+} spins, placing the onset of long-range antiferromagnetic correlations at $T_f < 11$ K. The intriguing feature of the $\text{Nb}_{12}\text{O}_{29}$ compound is that ZF- μ SR resolves two discrete frequencies $\nu_1 = 0.532(8)$ MHz and $\nu_2 = 1.873(14)$ MHz at 60 mK, corresponding to static local fields $\langle B_{\mu} \rangle$ at the muon site of 39.3(6) and 138(1) G, respectively. This is a manifestation of muons seeing distinct internal magnetic fields with

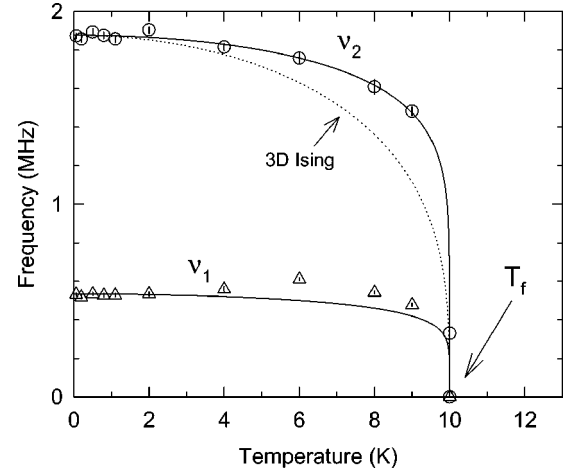


FIG. 4. Temperature dependence of the two spontaneous muon-spin precession frequencies close and below the antiferromagnetic ordering transition (T_f) in monoclinic $\text{Nb}_{12}\text{O}_{29}$. The solid lines are fits to a power-law behavior, with $\beta = 0.15(2)$ [Eq. (4)], and the dotted curve corresponds to 3D Ising critical behavior $\beta = 0.312$.

a constant magnitude because they appear static or quasi-static in the time scale of the μ SR experiment (i.e., over a few muon lifetimes). In $\text{Nb}_{12}\text{O}_{29}$ the muons experience static local fields with some spatial inhomogeneity, which becomes apparent in the ZF- μ SR spectra as additional broadening of the line shape. It can be caused due to the fact that the ordered moment locally experiences changes in magnitude and sign due to the incommensurate nature of the modulated spin structure. A measure of this is given by the size of the corresponding depolarization rates $\lambda_1 = 0.86(8) \mu\text{s}^{-1}$ and $\lambda_2 = 0.51(12) \mu\text{s}^{-1}$ at 60 mK, implying a distribution of local fields with a width $\langle \Delta B^2 \rangle^{1/2}$ of 10.1(9) and 6(1) G, respectively. Some of the physical reasons for this behavior will be discussed below on the basis of the structural arguments that hold for this reduced niobium oxide. The temperature variation of the two resolved muon-spin precession frequencies in $\text{Nb}_{12}\text{O}_{29}$ reflects the vanishing of the sublattice magnetization at T_f . This behavior is shown in Fig. 4, as we approach the spin-freezing temperature $T_f \approx 10$ K, and to a first approximation appears to be described by the following power law:

$$\nu = \nu_0 \left[1 - \left(\frac{T}{T_f} \right)^\delta \right]^\beta \quad (4)$$

with $\delta = 1.9(3)$ and $\beta = 0.15(2)$.¹² The parameter, β is a critical index, which describes the order parameter near the magnetic phase transition and depends on the type of the spin-spin coupling and its dimensionality (e.g., $\beta = 0.38$ for 3D Heisenberg, $\beta = 0.312$ for 3D Ising, $\beta = 0.124$ for 2D Ising models).¹³ On the other hand, δ is not a critical parameter but reflects magnon excitations, which have the tendency to suppress the order parameter at low temperatures. The sharp appearance of the frequency ν_{μ} is reminiscent of the spin-density-wave transitions in antiferromagnetic chromium¹⁴ or the charge-transfer salt $(\text{TMTSF})_2\text{X}_6$.¹⁵ Although there is a unique crystallographic site associated with

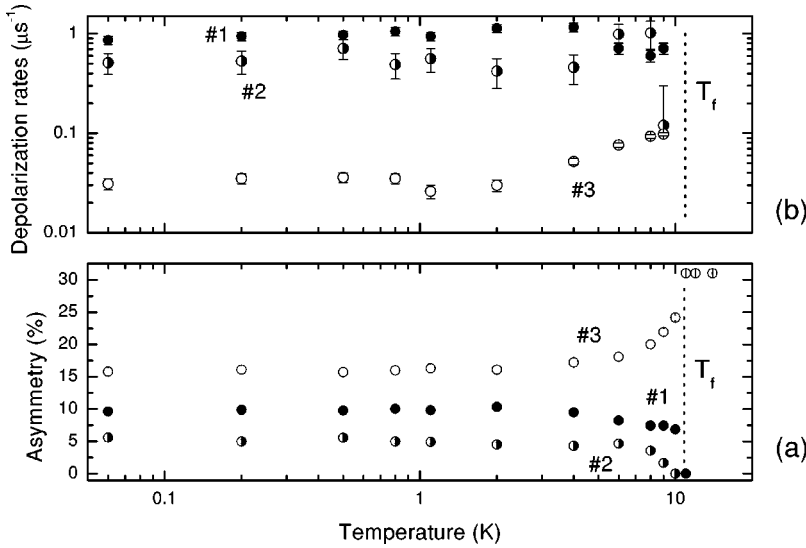


FIG. 5. The temperature dependence of (a) the zero-time asymmetries for the paramagnetic (No. 3) and magnetically ordered (Nos. 1, 2) volume fraction of muons participating in the relaxation mechanisms. (b) The associated relaxation rates. Equations (2) and (3) were employed in this description.

the ordering of the Nb⁴⁺ cations in the crystal lattice, justification of multiple frequencies can in general be made on the grounds of a complex magnetic system where there is more than one low-energy site for the muon to be located.

Our ZF- μ^+ SR data reveal clearly a cooperative magnetic transition. Figure 5(a) shows the temperature dependence of the corresponding fractions of the muons for each component in $P_\mu(t)$. The static magnetism which gives rise to the oscillating μ^+ -spin polarization first appears at $T_f \approx 10$ K. It is reflected in the asymmetries of components Nos. 1 and 2, namely A_1^\perp and A_2^\perp . This signal increases substantially at lower temperatures as the magnetically ordered domains grow at the expense of the paramagnetic ones whose volume fraction is hidden in parameter A_3^\parallel of the nonoscillating component No. 3. This latter contribution involves also the $\frac{1}{3}$ nonprecessing term of the magnetic component (due to the polycrystalline nature of the material), which cannot become disentangled from the truly paramagnetic domain fraction possibly due to the proximity of the relaxation rates for the two signals. The data imply a partly inhomogeneous form of magnetism for Nb₁₂O₂₉, with coexisting paramagnetic and ordered static ($\sim 74\%$) internal fields even down to 60 mK. The associated relaxation rates [Fig. 5(b)] do not, however, show the fairly strong temperature dependence of the amplitudes close to T_f .

The low-dimensional properties of the monoclinic Nb₁₂O₂₉ system are inherent in its crystal structure.⁴ The charge ordering in this compound effectively results in infinite one-dimensional Nb⁴⁺, $S = \frac{1}{2}$ chains of corner-shared NbO₆ octahedral units running down the b axis. These are confined within 2D planes, which are “cutting diagonally” through the 3×4 NbO₆ blocks, joined to one another by edge-sharing octahedra (Fig. 1). In terms of magnetic exchange interactions the adjacent 2D planes are isolated from one another, and in this case we can assume that the Nb₁₂O₂₉ system is composed of a 2D array of loosely coupled $S = \frac{1}{2}$ chains. If Nb₁₂O₂₉ was a purely one-dimensional solid then, as inferred from examples of simple magnetic model systems in real crystals,¹⁶ we would expect the thermodynamic behavior of such an 1D system to be governed by the intrinsic

property common to all of them, namely, the absence of long-range order at nonzero temperature. Theoretical investigations¹⁶ on the critical properties of such a 2D array of loosely coupled chains suggest that, close enough to the ordering temperature T_f , they are essentially the same as those of a quadratic lattice with a critical exponent $\beta \sim \frac{1}{8}$. The extracted index $\beta = 0.15(2)$ from the ZF- μ SR experiments, is in line with the spin-spin interactions originating from a 2D Ising-like model. In such a quasi-1D system, a weak but finite interchain interaction within the 2D planes, can establish long-range ordering. In Fig. 4 we also plot the calculated behavior for a 3D Ising model ($\beta = 0.312$), as approximated by 3D arrays of loosely coupled chains, with the same critical temperature T_f as for the current experiment. We can see that the less anisotropic the system, the faster the reduction of the sublattice magnetization.

We would like to note that although there is a single crystallographic Nb⁴⁺ site, the muons attracted at the most electronegative regions, can stop in various interstitial sites in the Nb₁₂O₂₉ lattice. It is likely that the complex shear plane structure of Nb₁₂O₂₉ will contain a number of inequivalent sites with similar attractive energies, each site giving rise to a distinct spontaneous μ^+ -spin precession frequency. For example, inspection of the crystal structure shows two candidate muon stopping sites; first the interstitials between the Nb⁴⁺ chains located in the 2D planes (“cutting diagonally” through the 3×4 NbO₆ blocks) and secondly in the corresponding interlayer space (Fig. 1). Muons located at each site will feel dipolar fields of varying strength, because of the different topology of the surrounding moment configurations. From neutron diffraction studies,⁴ it was found that each chain has six neighbors at distinctly different distances, four long ones at $r_1 \cong 15.7 \text{ \AA}$ ($\times 2$), 15.1 \AA ($\times 2$) and two shorter at $r_2 \cong 10.5 \text{ \AA}$ ($\times 2$). The lack of Knight-shift data, which offers a measure of the dipolar contribution at muon sites precludes accurate determination of the muon location. However, we can estimate whether the muon senses local fields from magnetically distinct sites based on the chain topological separation. The electronic dipole fields vary as $\langle B_\mu \rangle \sim \nu_\mu \sim 1/r^3$ from the site that the muon probes, there-

TABLE I. Exchange energies J/K for a number of one-dimensional molecular and condensed phase magnetic systems.

	J/K	Reference
Monoclinic Nb ₁₂ O ₂₉	12.71	This work
(VO) ₂ P ₂ O ₇	65.7	17
Sr ₂ Cu ₂ O ₃	2200	18
SrCuO ₂	2100	18
NaV ₂ O ₅	530	19
CsV ₂ O ₅	146	19
LiV ₂ O ₅	310	19
CuGeO ₃	121	20
[3,3'-dimethyl-2,2'-thiazolinocyanine] (TCNQ)	32.5	21
MEM-[TCNQ]	53	22
Cu diazocycloheptane Cl ₂	15.3	23, 24
Catena-[octanedione bis (thiosemicarbazonato)]copper(II)(Cu-OTS)	18.6	25
Catena-[hexanedione bis (thiosemicarbazonato)]copper(II) (Cu-HTS)	14.5	25
Cu(4-methylpyridine)Cl ₂	13.8	25
Dibromobis(thiazole)copper(II)	5.5	26
Dichlorobis(thiazole)copper(II)	15.0	26
LiCuCl ₃ ·H ₂ O	5.3	27
Isopropylammonium copper (II) trichloride	19.7	27

fore, the relation $\nu_1/\nu_2=(r_2/r_1)^3$ is a useful measure for exploring candidate muon sites. Using the experimentally observed values for the spontaneous μ^+ -precession frequencies and the distances for an average chain separation,⁴ we find $\nu_1/\nu_2=0.28(1)$ and $(r_2/r_1)^3=0.32$. This suggests that the muons occupy interstitial sites within a distance comparable to the real separation of the chains in the Nb₁₂O₂₉ crystal structure. This is consistent with the fact that, assuming

$r_1>r_2$, the Larmor frequency magnitudes have the relation $\nu_1<\nu_2$, as found experimentally.

We have shown through the use of magnetic susceptibility and zero-field μ^+ SR studies that the magnetic transition in monoclinic Nb₁₂O₂₉ is associated with a long-range antiferromagnetically ordered ground state. This is consistent with the ordering of the Nb⁴⁺ ions onto a distinct crystallographic site, which comprises a unique form of a one-dimensional magnet. The large distances between the NbO₆ chains (nearest neighbors at 15.7, 15.1, and 10.5 Å) preclude direct or superexchange type of interactions forming an exchange pathway for the magnetic correlations between the chains. However, the presence of distinct conduction electrons makes an indirect exchange through a sinusoidal varying RKKY interaction possible, consistent with the zero-field μ^+ SR measurements, yielding an incommensurate magnetic structure. This, together with the inherent low-dimensional character of the structure, results in a different topology for the surrounding moment configurations. The muons are located in at least two distinct interstitial sites and experience distinct dipolar fields [$\langle B_\mu \rangle = 39.3(6)$ and $138(1)$ G]. In contrast to other condensed phase material, Nb₁₂O₂₉ shows characteristics which are more associated with organic molecular magnets, including the charge-transfer salt (TMTSF)₂X₆.¹⁵ This is highlighted when we compare the exchange energies of a number of condensed phase and molecular magnetic systems, as shown in Table I. The flexibility of the condensed phase systems, such as Nb₁₂O₂₉, allows for sophisticated alteration of the number of arrangements of chains through intercalation and substitution experiments.

Financial support through the EPSRC and the European Science Exchange Programme of the Royal Society is acknowledged. We also thank the Paul Scherrer Institute for provision of muon beam time, A. Schenck for useful discussions and C. Baines for technical support with the μ^+ SR experiments.

*Email address: mark@ri.ac.uk

¹S.-W. Cheong, H.Y. Hwang, C.H. Chen, B. Batlogg, L.W. Rupp, Jr., and S.A. Carter, Phys. Rev. B **49**, 7088 (1994).

²S. Pei, J.D. Jorgensen, B. Dabrowski, D.G. Hinks, D.R. Richards, A.W. Mitchell, J.M. Newsam, S.K. Sinha, D. Vaknin, and A.J. Jacobsen, Phys. Rev. B **41**, 4126 (1990).

³For a review see C.N. Rao, A. Arulraj, P.N. Santosh, and A.K. Cheetham, Chem. Mater. **10**, 2714 (1998).

⁴J.E.L. Waldron, M.A. Green, and D.A. Neumann, J. Am. Chem. Soc. **123**, 5833 (2001).

⁵R.J. Cava, B. Batlogg, J.J. Krajewski, P. Gammel, H.F. Poulson, W.F. Peck, and L.W. Rupp, Nature (London) **350**, 598 (1991).

⁶J.A. Mydosh, *Spin Glasses: An Experimental Introduction* (Taylor and Francis, London, 1993).

⁷D. Jérôme, in *Organic Conductors: Fundamentals and Applications*, edited by J.P. Farges (Dekker, New York, 1994).

⁸A. Schenck and F.N. Gyax, in *Handbook of Magnetic Materials*, edited by K.H.J. Buschow (Elsevier, New York, 1995), Vol. 9, pp. 57–301.

⁹J.C. Bonner, Ph.D. thesis, University of London, 1968.

¹⁰S. Barth, H.R. Ott, F.N. Gyax, B. Hitti, E. Lippelt, A. Schenck, and C. Baines, Phys. Rev. Lett. **59**, 2991 (1987).

¹¹Y.J. Uemura, T. Yamazaki, D.R. Harshman, M. Senba, and E.J. Ansaldo, Phys. Rev. B **31**, 546 (1985).

¹²J.J. Binney, N.J. Dowrich, A.J. Fischer, and M.E.J. Newman, in *The Theory of Critical Phenomena* (Oxford University Press, Oxford, 1992).

¹³A. Schenck, in *Muon Science: Muons in Physics, Chemistry and Materials*, edited by S.L. Lee, S.H. Kilcoyne, and R. Cywinski (Institute of Physics, London, 1999), p 75.

¹⁴A. Arrot, S.A. Werner, and H. Kendrick, Phys. Rev. Lett. **14**, 1022 (1965).

¹⁵L.P. Le, A. Keren, G.M. Luke, B.J. Sternlieb, W.D. Wu, Y.J. Uemura, J.H. Brewer, T.M. Riseman, R.V. Upasani, L.Y. Chiang, W. Kang, P.M. Chaikin, T. Csiba, and G. Gruner, Phys. Rev. B **48**, 7284 (1993).

¹⁶See Sec. 3.1 of L.J. de Jongh and A.R. Miedema, Adv. Phys. **23**, 1 (1974).

¹⁷D.C. Johnson, J.W. Johnson, D.P. Goshorn, and A.J. Jacobson, Phys. Rev. B **35**, 219 (1987).

- ¹⁸N. Moyotama, H. Eisaki, and S. Uchida, Phys. Rev. Lett. **76**, 3212 (1996).
- ¹⁹Y. Ueda, Chem. Mater. **10**, 2653 (1998).
- ²⁰M.A. Green, M. Kurmoo, J.K. Stalick, and P. Day, J. Chem. Soc. Chem. Commun. **1994**, 1995.
- ²¹S. Takagi, H. Deguchi, K. Takeda, and M. Mito, J. Phys. Soc. Jpn. **65**, 1934 (1996).
- ²²S. Huizinga, J. Kommandeur, G.A. Sawatzky, B.T. Thole, K. Kopinga, W.M.J. de Jonge, and J. Roos, Phys. Rev. B **19**, 4723 (1979).
- ²³P.R. Hammar and D.H. Reich, J. Appl. Phys. **79**, 5392 (1996).
- ²⁴P.R. Hammar, D.H. Reich, C. Broholm, and F. Trouw, Phys. Rev. B **57**, 7846 (1998).
- ²⁵J.W. Hall, W.E. Marsh, R.R. Weller, and W.E. Hatfield, Inorg. Chem. **20**, 1033 (1981).
- ²⁶W.E. Estes, D.P. Gavel, W.E. Hatfield, and D.J. Hodgson, Inorg. Chem. **17**, 1415 (1978).
- ²⁷L.W.t. Haar and W.E. Hatfield, Inorg. Chem. **244**, 1022 (1985).